Self-Assembly, Characterisation, and Crystal Structure of Multinuclear Metal Complexes of the [2 × 3] and [3 × 3] Grid-Type

Esther Breuning,[a] Garry S. Hanan,[a] Francisco J. Romero-Salguero,[a] Ana M. Garcia,[a] Paul N. W. Baxter,[a] Jean-Marie Lehn,*[a] Elina Wegelius,[b] Kari Rissanen,[b] Hélène Nierengarten,[c] and Alain van Dorsselaer[c]

Abstract: The self-assembly of new multimetallic complexes of grid-type architecture is described. The binding of a set of tris-terdentate ligands, **1a**–**1d**, based on terpyridine-like subunits, with different octahedrally coordinated metal ions leads to the formation of species whose structure depends strongly on the ligand, the metal ion, the counterion, the solvent, and the reaction conditions. Under suitable conditions, the [3 × 3] grid was obtained from the reaction of ligand **1a** with zinc tetrafluoroborate and from ligand **1b** with mercury triflate. The other ligands led to the formation of mainly one compound of composition $[M_6L_5]^{12+}$, which has the structure of an incomplete [2 × 3] grid. The crystal structure of such a [2 × 3] grid, $[Co_6(\mathbf{1d})_5]^{12+}$, has been determined. In this complex, the three central pyrimidine—pyridine–pyrimidine non-coordinating sites adopt *transoid* NC–CN conformations. The much less stable *cisoid* conformations, the "pinching" of the coordination sites in the complex, the weaker donor strength of the central binding site, and the steric demand of the substituents are all factors contributing to the reluctance to produce the [3 × 3] structure. A subtle interplay between the nature of the metal, the steric demand of the ligand, the reaction conditions, and the type of counterion determine the product of self-assembly. The results obtained show that by tuning the parameters, complexes containing six or nine octahedrally coordinated metal ions in a well-defined grid-type arrangement are accessible. Both types of arrays, [2 × 3] and [3 × 3], are of interest as self-assembled inorganic architectures of well-defined structure and nuclearity that may be suitable prototypes for selective information storage media.

Keywords: coordination chemistry · grid-type compounds · N ligands · self-assembly · supramolecular chemistry

Introduction

During the last few years, intense investigations have been carried out on the generation of complex inorganic architectures by self-assembly from their components.[1] One fundamental type of polypyridine-derived coordination array has recently been described: [*m* × *n*] grid-type complexes[2] where the nuclearity of the compound is given by [*mn*] (Scheme 1).

The first complexes of grid-type architecture employed bipyridine-like binding subunits and the tetrahedrally coordinated metal ions Cu^I and Ag^I.[2a–c] This kind of architecture was then extended to [2 × 2] grids of octahedrally coordinated

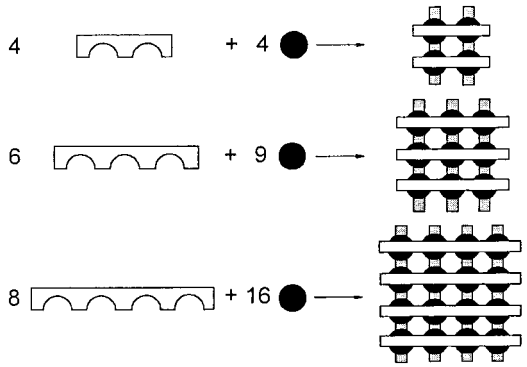

Scheme 1. Schematic representation of the self-assembly process of [2 × 2], [3 × 3] and [4 × 4] grid-type architectures.

[a] Prof. J.-M. Lehn, Dr. E. Breuning, Dr. G. S. Hanan, Dr. F. J. Romero-Salguero, Dr. A. M. Garcia, Dr. P. N. W. Baxter
Laboratoire de Chimie Supramoléculaire
ISIS-Université Louis Pasteur
4, rue Blaise Pascal, 67000 Strasbourg (France)
Fax: (+33) 3-90-24-11-17
E-mail: lehn@chimie.u-strasbg.fr

[b] Dr. E. Wegelius, Prof. K. Rissanen
Department of Chemistry, University of Jyväskylä
P.O. Box 35, FIN-40351 Jyväskylä (Finland)

[c] Dr. H. Nierengarten, Dr. A. van Dorsselaer
Laboratoire de Spectrométrie de Masse Bio-Organique
Université Louis Pasteur, CNRS UMR 7509, ECPM
25 rue Becquerel, 67087 Strasbourg cedex 2 (France)

  0947-6539/02/0815-3458 $ 20.00+.50/0

first-row transition metal ions such as Co^{II}, Ni^{II}, Zn^{II} and ligands based on terpyridine-like binding sites.[2d] These complexes present remarkable physical (such as electronic,[3] magnetic,[4] and photophysical[5]) properties. It has also been demonstrated that they can be arranged regularly on a surface and observed and manipulated on a single unit level by scanning tunneling microscopy (STM).[6]

Recently, grid-type complexes containing nine octahedrally coordinated metal ions in a $[3 \times 3]$ arrangement were obtained, using a new ligand system to build up the grid-like coordination compounds.[7] These complexes show magnetic coupling between the metal centres, and interesting redox properties. So far, grid-type complexes of higher nuclearity than $[2 \times 2]$, based on our ligands, employed only tetrahedrally coordinated cations Cu^{I} and Ag^{I} (up to 20 ions)[2b,c] and octahedrally coordinated Pb^{II} (16 ions).[8] However, the latter metal ions do not present the palette of magnetic or electronic properties displayed by transition metal ions.

The success in the formation of grids of the $[2 \times 2]$ type as well as their highly interesting physical properties stimulated us to extend the synthesis towards grids of higher nuclearity based on octahedrally coordinated transition metal ions.

We report here on investigations of self-assembly processes involving tris-terdentate ligands **1a–d** (Scheme 2) based on terpyridine-like binding sites and the octahedrally coordinated metal ions Zn^{II}, Co^{II}, Fe^{II}, Cu^{II} and Hg^{II}. The ligand syntheses have been reported elsewhere.[9] These ligands **1a–d** bear three different substituents in the 2-position of the pyrimidine rings: hydrogen, methyl and phenyl. In addition, they are either unsubstituted on the outer rim or substituted by thiopropyl groups in the 4-positions of the three internal pyridine rings.

Abstract in French: *L'auto-assemblage de nouveaux complexes polymétalliques ayant une architecture en "grille" est décrit. La complexation des ligands tris-terdentates **1a–1d**, contenant des sites de type terpyridine, par des ions métalliques à coordination octaédrique conduit à la formation d'espèces dont la structure dépend fortement du ligand, de l'ion métallique, du contre-ion, du solvant et des conditions réactionnelles. Dans des conditions appropriées, la grille [3 × 3] a été obtenue à partir de la réaction du ligand **1a** avec le tetrafluoroborate de zinc et du ligand **1b** avec le triflate de mercure. Les autres ligands ont conduit principalement à la formation d'un composé ayant la composition $[M_6L_5]^{12+}$ qui possède la structure d'une grille incomplète [2 × 3]. La structure cristalline d'un complexes de ce type, $[Co_6(\mathbf{1d})_5]^{12+}$ a été déterminée. Dans ce composé, les trois sites internes pyrimidine-pyridine-pyrimidine non-coordinnés adoptent des conformations NC−CN transoides. Les conformations cisoides beaucoup moins stables, le pincement des sites de coordination dans le complexe, le caractère donneur plus faible du site central et les exigences stériques des substituants sont tous des facteurs défavorisant la formation d'une structure [3 × 3]. La nature du produit d'auto-assemblage résulte d'un délicat équilibre entre la nature du métal, les caractéristiques stériques du ligand, les conditions de réactions et le type de contre-ion. Les résultats obtenus montrent qu'en ajustant les paramètres, il est possible d'obtenir des complexes contenant six ou neuf ions métalliques coordinnés de façon octaédrique dans des arrangements de type grille clairement définis. Les deux types de réseau, [2 × 3] et [3 × 3] représentent des architectures inorganiques auto-assemblées de structure et de nucléarité bien définies, pouvant servir de prototypes pour le stockage sélectif d'information.*

Results and Discussion

Synthesis of metal complexes of the $[2 \times 3]$ and $[3 \times 3]$ grid-type: For the self-assembly of the complexes, 1.5 equivalents of the triflate, acetate or tetrafluoroborate metal salt, that is, the stoichiometric amount for the anticipated $[3 \times 3]$ grid structure (Scheme 2), was allowed to react with the ligand **1** at concentrations between 7 and 11 mM (in most of the cases) in different solvents and at different temperatures. The reaction conditions and results are summarised in Table 1.

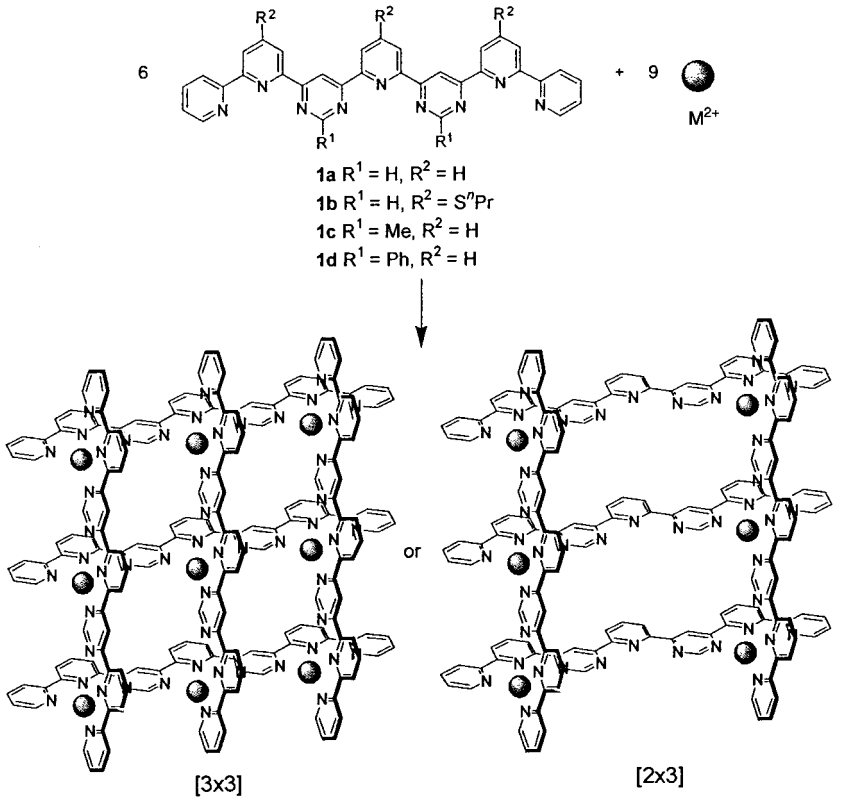

Scheme 2. Schematic representation of the self-assembly of a $[3 \times 3]$ grid (left) and a $[2 \times 3]$ grid (right) from the tritopic ligands **1a–d** and octahedrally coordinated metal ions (the substituents R^1 and R^2 in the grids are omitted for clarity; for the assembly of the $[2 \times 3]$ grid, only the energetically less favourable *cisoid* isomer is shown.

  0947-6539/02/0815-3459 $ 20.00+.50/0

Table 1. Reaction conditions and reaction products for the complexation of tris-terdentate ligands **1a**–**d** with different metal salts.[a]

L	Metal salt	Solvent	Conditions	Main products	Side products
1a	$Co(BF_4)_2 \cdot 6H_2O$	CH_3CN	18 h, reflux	$[2\times3]$	$[3\times3] + [2\times2]$
1a	$Zn(OAc)_2 \cdot 2H_2O$	MeOH	12 h, reflux	$[2\times3]$	none
1a	$Zn(OTf)_2 \cdot H_2O$	CH_3CN	21 h, reflux	$[2\times3]$	$[2\times2]$
1a	$Zn(BF_4)_2 \cdot 8H_2O$	CH_3CN	19 h, reflux	$[3\times3]$	none
1b	$Cu(OTf)_2$	$CH_3CN/CHCl_3$	48 h, RT	not interpretable	$[2\times3] + [2\times2]$
1b	$[Co(DMSO)_6](OTf)_2$	CH_3CN	48 h, reflux	$[2\times3]$	$[2\times2]$
1b	$Hg(OTf)_2$	CH_3CN	12 h, RT	$[3\times3]$	none
1c	$Co(BF_4)_2 \cdot 6H_2O$	CH_3CN	5 days, reflux	$[2\times3] + [2\times2]$	none
1c	$Co(BF_4)_2 \cdot 6H_2O$	benzonitrile	67 h, 180 °C	$[2\times3]$	$[2\times2]$
1c	$Fe(BF_4)_2 \cdot 6H_2O$	CH_3CN	5 days, reflux	$[2\times2]$	$[2\times3]$
1c	$Fe(BF_4)_2 \cdot 6H_2O$	benzonitrile	66 h, 180 °C	$[2\times3]$	$[2\times2]$
1c	$Zn(OTf)_2 \cdot H_2O$	CH_3CN	5 days, reflux	not interpretable	$[2\times3] + [2\times2]$
1c	$Zn(BF_4)_2 \cdot 8H_2O$	CH_3CN	19 h, reflux	$[2\times3] + [2\times2]$	none
1d	$Co(BF_4)_2 \cdot 6H_2O$	CH_3CN	23 days, reflux	$[Co(\mathbf{1d})]^{2+}$	$[2\times3] + [2\times2]$
1d	$Co(BF_4)_2 \cdot 6H_2O$	benzonitrile	20 h, 180 °C	$[2\times3]$	little $[2\times2]$
1d	$Fe(BF_4)_2 \cdot 6H_2O$	CH_3CN	16 days, reflux	$[Fe_6(\mathbf{1d})_6]^{12+}$	$[2\times3] + [2\times2] + [Fe(\mathbf{1d})]^{2+}$
1d	$Fe(BF_4)_2 \cdot 6H_2O$	benzonitrile	20 h, 180 °C	$[2\times3]$	$[2\times2]$
1d	$Zn(BF_4)_2 \cdot 8H_2O$	CH_3CN	4 days, reflux	$[2\times3]$	$[2\times2]$
1d	$Zn(OTf)_2 \cdot H_2O$	CH_3CN	6 days, reflux	$[Zn(\mathbf{1d})]^{2+}$	little $[2\times2] + [2\times3]$

[a] Concentration in most cases between 7 and 11 mM.

Inspection of the results (Table 1) revealed several general trends.

1) In most cases examined, $[2\times3]$ hexanuclear grids were generated in the reaction mixture and in the majority of examples constituted the major product.[10]
2) The reactions employing the less sterically hindered ligands **1a** and **1b** occurred readily under comparatively mild conditions, such as room temperature or reflux in acetonitrile. Reaction in nitromethane, which is the solvent of choice for Ag^I or Cu^I grids, did not result in grid-like products in our case, but only in smaller fragments. The complexes were isolated by evaporation of the solvent. For the Zn^{II} complex of **1a**, the acetate salt in methanol was also used. In this case, the complex was isolated from the reaction mixture by precipitation after anion exchange with ammonium hexafluorophosphate.
3) Ligands possessing sterically demanding substituents in the 2-position of the pyrimidine in **1c** and **1d** made the progression of the reaction towards thermodynamic equilibrium more difficult. Thus, heating under reflux in acetonitrile resulted in mixtures of different products, whereas mainly one compound was obtained when the reaction was performed at 180 °C in benzonitrile. In this case, the products were isolated by precipitation with diethyl ether. The different reaction outputs are illustrated by two electrospray ionisation (ESI) mass spectra shown in Figure 1, which correspond to the reaction of **1d** with $Co(BF_4)_2 \cdot 6H_2O$ in acetonitrile under reflux (Figure 1a) and in benzonitrile at 180 °C (Figure 1b). Reaction in acetonitrile produced mixtures of grids (accompanied by smaller fragments and a hexanuclear species, see below), whereas reaction in benzonitrile resulted in the mainly pure $[2\times3]$ grid. The same trend was observed with **1d** and $Fe(BF_4)_2 \cdot 6H_2O$, as well as with ligand **1c**.

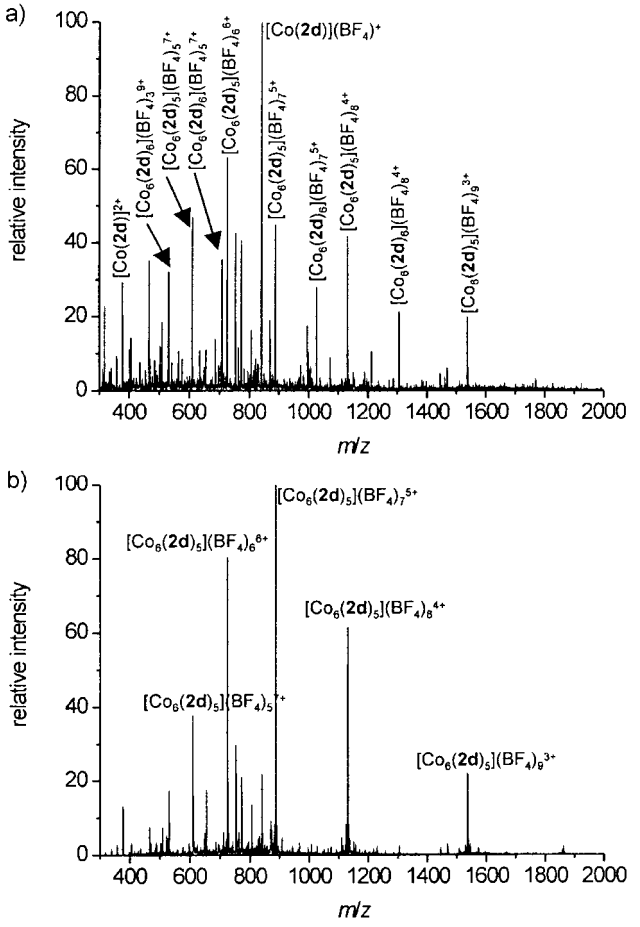

Figure 1. ESI mass spectrum of the product of reaction of **1d** with $Co(BF_4)_2 \cdot 6H_2O$ in acetonitrile under reflux (a) and in benzonitrile at 180 °C (b).

Characterisation by ^1H NMR spectroscopy (see below) and ESI-MS showed that in most cases the reaction mixture contained mainly one product of the composition $[M_6L_5]^{12+}$, which could be a $[2\times3]$ grid-type complex with two of the edges fully coordinated and three inner sites unoccupied (Schemes 2 and 3). This is often accompanied by a secondary product of composition $[M_4L_4](X)_8$, probably of $[2\times2]$ grid structure with all central binding sites non-coordinating

  0947-6539/02/0815-3460 $ 20.00+.50/0 *Chem. Eur. J.* **2002**, *8*, No. 15

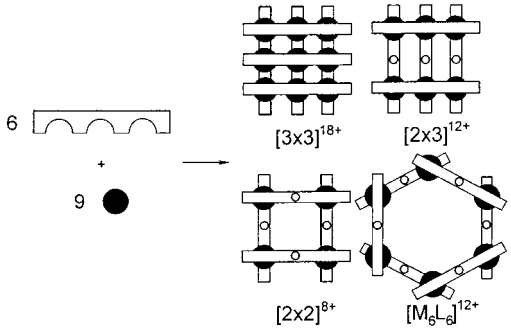

Scheme 3. Different possible reaction outputs from the reaction of ligand **1** with octahedrally coordinated metal ions. The uncomplexed terpyridine type sites are noted by an open circle; they should adopt a *transoid–transoid* arrangement (see Scheme 4).

(Scheme 3). The non-coordinating sites are expected to adopt a *transoid* conformation about the central NC–CN bonds (Scheme 4), which is calculated to be about 25 – 30 kJ mol^{-1} more stable than the *cisoid* one.[11, 12] However, it is not

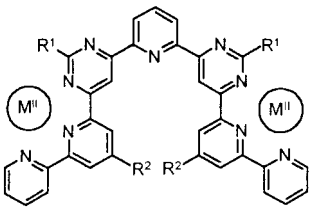

Scheme 4. Assumed conformation of ligand **1** in incomplete [2 × 3] and [2 × 2] grid structures, with a *transoid–transoid* conformation around the two C–C bonds of the central terpyridine-type unit.

possible to distinguish between the two conformations by ESI-MS, and the distinction by NMR spectroscopy is often ambiguous. Therefore, a general conclusion is only possible by comparison with a single-crystal structure (see below). The reaction of ligand **1d** with $Fe(BF_4)_2 \cdot 6H_2O$ in acetonitrile under reflux did not lead to a grid-type structure as main product, but a species of composition $[Fe_6(\mathbf{1d})_6](BF_4)_{12}$. We assume that this product is of hexagonal geometry (Scheme 3) with all central binding sites non-coordinating and in a *transoid* conformation, but so far no single crystals have been obtained.

Reaction of ligand **1b** with $Cu(OTf)_2$ resulted in a product, which, according to ESI-MS, appears to be a mixture of the [2 × 3] Cu^{II}_6 grid together with an unidentified other product.

The reaction of **1a** with zinc triflate, zinc acetate and zinc tetrafluoroborate revealed the profound influence of the counterions. The same trend was observed for ligands **1c** and **1d**. With the triflate salt in acetonitrile, smaller complex fragments were in general formed, or the composition of the main reaction product could not be assigned at all. The reaction of **1a** with zinc triflate and zinc acetate, for example, resulted in the [2 × 3] grid with some [2 × 2] grid as side product. Reaction of **1a** with the tetrafluoroborate salt, however, formed the pure [3 × 3] grid. The ESI mass spectrum of $[Zn_9(\mathbf{1a})_6](BF_4)_{18}$ is depicted in Figure 2. It shows only the presence of pseudomolecular peaks of the [3 × 3] grid corresponding to successive loss of tetrafluoroborate counter-

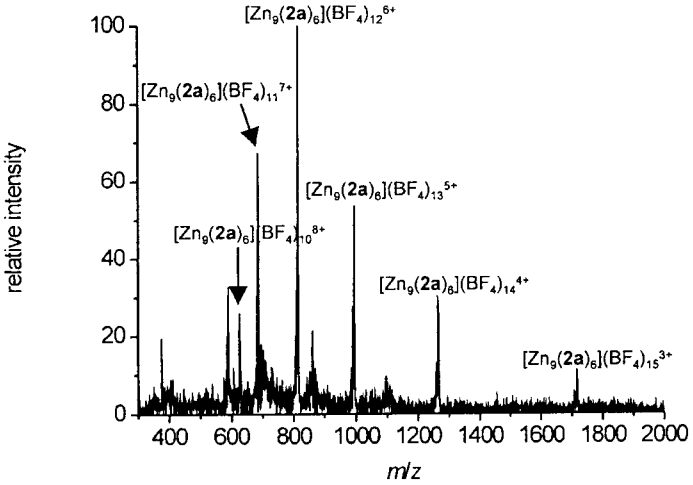

Figure 2. ESI mass spectrum of $[Zn_9(\mathbf{1a})_6](BF_4)_{18}$.

ions. The difference in reactivity with the three zinc salts may be attributed to the different coordinative properties of the triflate, the acetate and the tetrafluoroborate anion. The more strongly coordinating triflate or acetate are possibly in competition with the ligand for the metal ion. This may result in smaller fragments of the grid with free coordination sites of the metal occupied by triflate or acetate anions. Anion-templating effects in the case of the [2 × 3] and [2 × 2] grid complexes may also play a role.[13]

In the reaction of $Hg(OTf)_2$ with **1b**, the [3 × 3] grid-type complex was isolated as the main reaction product. The increased ionic radius of Hg^{II} ($R_i = 1.16$ Å) compared to that of the other metal ions used in this study ($R_i(Fe^{II}) = 0.75$ – 0.92, $R_i(Co^{II}) = 0.89$, $R_i(Cu^{II}) = 0.87$, $R_i(Zn^{II}) = 0.88$ Å)[14] probably reduces the pinching[15] of the ligand and results in a less strained grid architecture. This is also consistent with the fact, that the [4 × 4] grid of the Pb^{II} ion ($R_i = 1.33$ Å) is readily accessible.[8]

The reason why the [3 × 3] grid is not the most stable entity in the majority of cases may originate from a reluctance to produce a structure that:

1) has all the ligands in the *cisoid* conformation about the central NC–CN bonds, which is less stable when uncoordinated,
2) has a bent shape in two perpendicular directions ("pinching-in" of the ligand),[15] and
3) possesses a central metal ion coordinated by four pyrimidine nitrogen atoms, which are poorer donor atoms, and only two pyridine nitrogen atoms, compared to four or three pyridine and two or three pyrimidine nitrogen atoms for the corner and edge binding sites, respectively. This effect has also been noted earlier[2b,c] and results in unusually long M–N bond lengths for the central metal ion of the [3 × 3] grid, a factor which destabilises its structure and mitigates against its formation.

As noted above, the steric demand of the substituents in the 2-position of the pyrimidine rings in ligands **1c** and **1d** appear to prevent the formation of the [3 × 3] structure. This becomes evident as the Zn^{II}_9 [3 × 3] grid forms readily with ligand **1a**, but not with ligand **1c** or **1d**. However, the presence of methyl or phenyl substituents in the 2-position of the pyrimidine rings

would help releave the "pinching effect" noted above. A subtle interplay between ligand and metalions as well as between thermodynamic and kinetic factors determines the resulting supramolecular architectures. A detailed investigation into the reaction pathway leading to the formation of the $[M_9L_6]^{18+}$ grids will be necessary in order to resolve this issue.

Characterisation of the grid complexes by NMR spectroscopy: The difference between the complexes formed by reaction of **1a** with $Zn(OAc)_2$ and $Zn(BF_4)_2 \cdot 8H_2O$ becomes evident from their proton NMR spectra.

[Zn$_6$(1a)$_5$](PF$_6$)$_{12}$: The ^{1}H NMR spectrum of the Zn complex of **1a**, which was formed by reaction with $Zn(OAc)_2$ followed by anion exchange with NH_4PF_6 (Figure 3), displays a total of 33 signals in a 2:2:1 ratio between corresponding protons, along with minor impurities. The ring position of the protons were obtained by an $^1H-^1H$ COSY (Figure 3) experiment and the relative positions of the protons along the ligand backbone by an ^{1}H ROESY experiment. The formulation most consistent with the NMR data is that of a $[2 \times 3]$ grid $[Zn_6(\mathbf{1a})_5]^{12+}$ complex with the central terdentate sites of three ligand strands of **1a** uncomplexed.

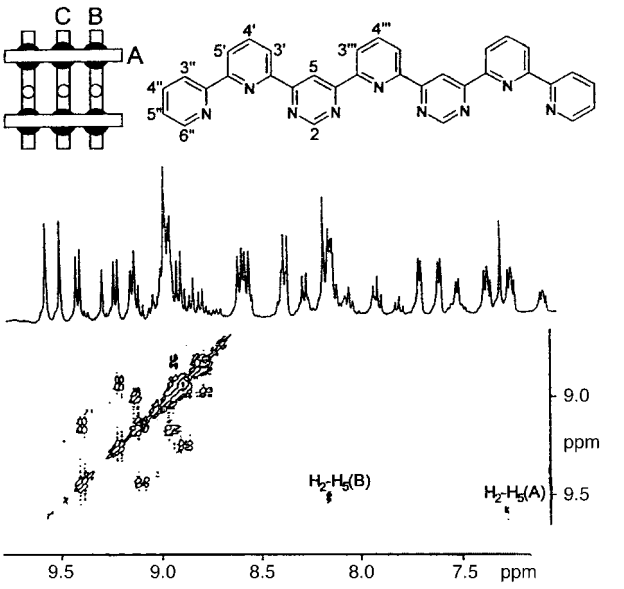

Figure 3. ^{1}H NMR spectrum and $^1H-^1H$ COSY spectrum of $[Zn_6(\mathbf{1a})_5](PF_6)_{12}$ in CD_3CN (400 MHz, 298 K) and labelling scheme of the complex. The three ligands B, C, B are expected to be in the conformation represented in Scheme 4.

There are two units of **1a** representing strands A, located on the outer coordination subunits of strands B and C and having all their terdentate sites filled. The ligand backbone of strand A is lined up and has interannular NOE interactions along its length. Two units of **1a** form strands B, located on the outer edges of strand A. Their central coordination sites are not occupied. The central pyridine and the two flanking pyrimidines should be in a *transoid* arrangement about the C–C bonds connecting the heterocycles. The single strand C occupies the central coordination site of strands A. The integrations of the peaks should be 2:2:1 for strand A:B:C, respectively, in agreement with the observed signals. The assignment of strand C was straightforward as each peak integrated to half of its counterpart from the remaining two strands. The H_5 proton signals, also presenting a 2:2:1 ratio, are all found in the low field end of the spectrum. The relationship between H_2 and H_5 is found in the COSY spectrum for strands A and B (Figure 3). The central pyridine protons $H_{3''}$(A) and $H_{4'''}$(A) are in an environment different from that of strands B and C as indicated by the difference in chemical shift. They are overlapping with the protons on the other heterocyclic rings of the strand as a result of the change to *cisoid* nitrogen conformation upon coordination to three metal ions. The ^{1}H ROESY spectrum reveals that the doublet assigned as H_5(A) has two NOE interactions to nearby protons. These protons may be assigned to $H_{3''}$(A) and $H_{3'}$(A) for the reasons stated above. The two lower field H_5 protons partake in only one NOE interaction, each with the nearby $H_{3'}$ protons. Further NOE interactions between $H_{5'}$ and $H_{3''}$ complete the connectivity of the rings in strand A. NOE interactions between $H_{5'}$ and $H_{3''}$ for strands B and C were not observed, although, regardless of whether the central pyridine nitrogen atom is *transoid* to the pyrimidine or not, an $H_{3'}-H_{3''}$ NOE interaction for strand B and C should be present.

[Zn$_9$(1a)$_6$](BF$_4$)$_{18}$: The ^{1}H NMR spectrum of the reaction product of **1a** with $Zn(BF_4)_2 \cdot 8H_2O$ is quite different from the spectrum of $[Zn_6(\mathbf{1a})_5](PF_6)_{12}$ described above. It displays a total of 22 peaks in a 2:1 ratio as expected for the external to internal ligand of a symmetrical $[3 \times 3]$ complex, $[Zn_9(\mathbf{1a})_6](BF_4)_{18}$, along with minor impurities (Figure 4).

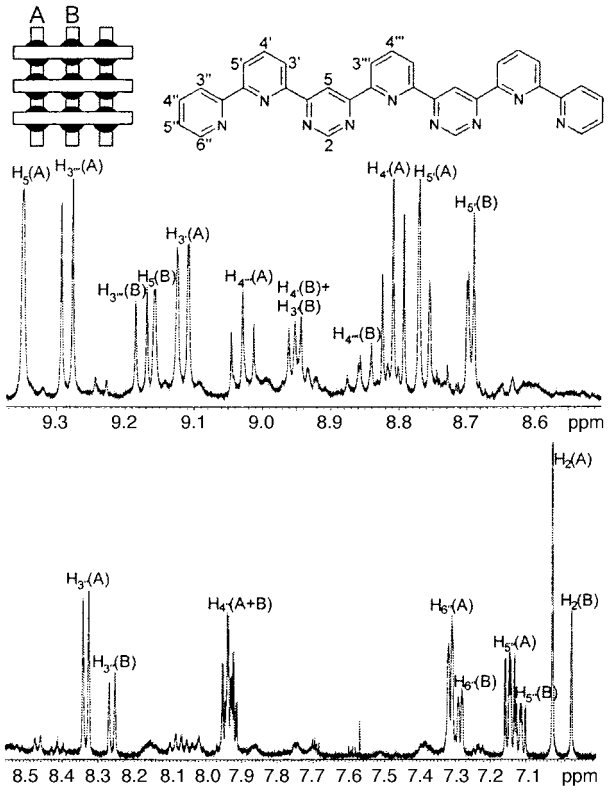

Figure 4. ^{1}H NMR spectrum of $[Zn_9(\mathbf{1a})_6](BF_4)_{18}$ in CD_3CN (500 MHz, 298 K) and labelling scheme of the complex.

0947-6539/02/0815-3462 $ 20.00+.50/0 *Chem. Eur. J.* **2002**, *8*, No. 15

The ring positions of the protons were obtained by a $^1H-^1H$ COSY experiment and the relative positions of the protons along the ligand backbone were determined by a ^1H NOESY experiment. It can therefore be concluded that the Zn^{II}_9 [3 × 3] grid was formed as the main reaction product. There are four units of **1a** representing ligand strand A. They make up the outer rim of the [3 × 3] grid. Strands B with two units of **1a** occupy the central sites. The assignment of ligand A and B both in the high field as well as in the low field part of the spectrum is straightforward as each signal of ligand B integrates to half of that of its counterpart from strand A. A few crosspeaks expected in the $^1H-^1H$ COSY spectrum were actually not present, however, as these signals were expected in close proximity to the diagonal, their absence is probably due to noise in the projection of the spectrum on the diagonal. The NOESY spectrum of $[Zn_9(\mathbf{1a})_6](BF_4)_{18}$ reveals the connectivity of the rings and allows final identification of the obtained species as a [3 × 3] grid. For both different ligands in the grid, there are NOE interactions between $H_{3''}$ and $H_{5'}$ and between $H_{3'}$ and H_5. This points to a *cisoid* conformation of the two terpyridine-like binding sites at the edges of the ligand. However, a further expected NOE between H_5 and $H_{3'''}$, which would prove the complete *cisoid* alignment of the ligand, was not observed in the spectrum. This crosspeak is expected to lie close to the diagonal of the spectrum so that it may not be resolved.

***Co, Fe and Cu complexes*:** For the paramagnetic Cu^{II} complex, no NMR spectrum could be recorded. In the case of the paramagnetic complexes of Co^{II} and Fe^{II} (Fe^{II} is in the paramagnetic high-spin state in complexes of ligands **1c** and **1d**) easily assignable NMR spectra were also unobtainable due to the signals being spread over several hundred ppm and accompanying loss of coupling information due to low resolution. The high number of signals, though, indicates that these complexes cannot be symmetrical [3 × 3] grids, but rather some less symmetrical species, which were subsequently identified as [2 × 3] grid-type complexes by ESI-MS. The presence of side products often complicates the interpretation of the spectra.

Crystal structure determination of $[Co_6(\mathbf{1d})_5](BF_4)_{12}$: Crystals of $[Co_6(\mathbf{1d})_5](BF_4)_{12}$ were obtained from acetonitrile/diisopropyl ether. The crystal structure analysis revealed that the constituent cations were indeed that of strikingly shaped [2 × 3] grid, in which five ligand components of **1d** are held together by six Co^{II} ions (Figure 5).

The overall shape of the cation as viewed perpendicularly to its mean plane through the six Co cations is that of a ladder with three rungs with a total size of approximately 24 × 25 Å. The five ligands are arranged into two sets, the first of which consists of three parallel ligands at a distance of 6.7 Å, which make up the three 'rungs' of the ladder. The ligands within this set are twisted into a *transoid* conformation about the two central pyrimidine–pyridine–pyrimidine C–C bonds, such that the central binding site of each is non-coordinating. The remaining nitrogen atoms form two terpyridine-like binding sites, which are coordinated to one cobalt ion each. The phenyl substituents of each ligand are in π-stacking contact

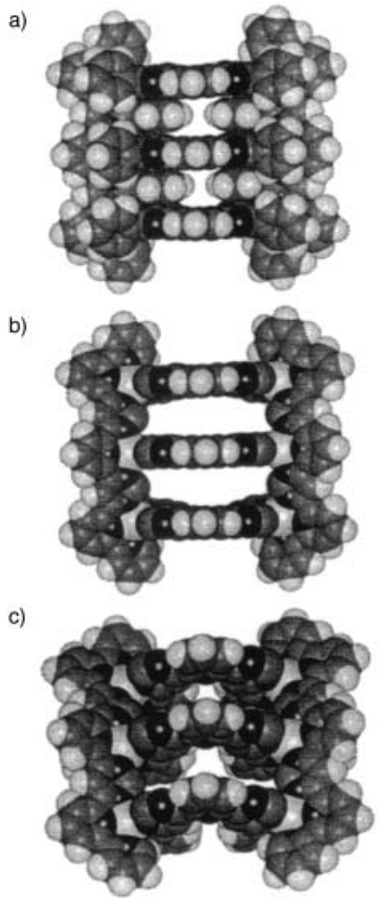

Figure 5. Single-crystal structure of $[Co_6(\mathbf{1d})_5]^{12+}$: a) and b) top view of the complex (with and without the phenyl rings, respectively), c) diagonal view (without phenyl rings) (anions and solvent molecules have been omitted for clarity).

(3.4–3.5 Å) with the heterocyclic rings of the perpendicularly arranged ligands. A single ligand from this set together with the coordinated Co ions is represented in Figure 6a and b. The

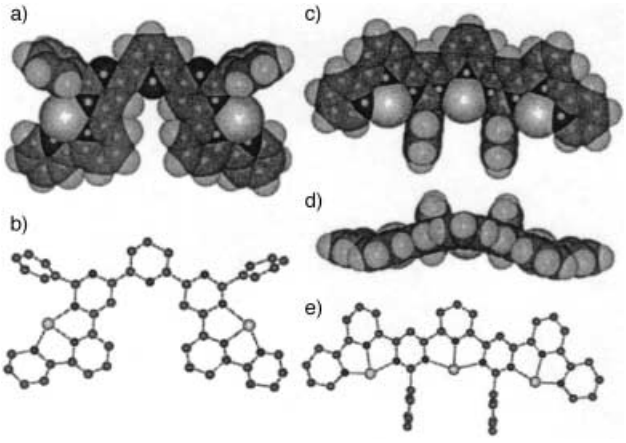

Figure 6. a) Space-filling representation of one of the three ditopic ligands as found in the crystal of the [2 × 3] grid $[Co_6(\mathbf{1d})_5]^{12+}$, illustrating the *transoid* conformation about the central pyrimidine–pyridine–pyrimidine C–C bonds and b) ball-and-stick representation; c) space-filling representation of one of the two tritopic ligands as found in the crystal, illustrating the all-*cisoid* conformation and the distortion of the ligand; d) warping of the ligand in *cisoid* conformation, space-filling representation, and e) ball-and-stick representation.

second ligand set is composed of two units of **1d** whose nitrogen atoms are fully coordinated and in a *cisoid* conformation about the connecting NC–CN bonds (Figure 6c–e). These ligands are not parallel to each other, but make an angle of 145° for the two outer binding sites and of 109° for the central binding site. This angle between the two ligands is imposed by the *transoid* conformation of the first ligand set. The difference between the angles for the outer and the central binding site reflects clearly the strong distortion of the ligand, which is no longer planar, but is markedly warped (Figure 6d). The phenyl rings of this ligand set insert between two perpendicular ligands of the former ligand set with double π-stacking contact (3.4 Å).

The Co ions are arranged into two rows of three ions. The ions in each row form an angle of 156°. The four corner Co^{II} ions describe a rectangle with Co–Co separations of 12.6 Å (for the side with three Co ions) and 13.8 Å (for the side with two Co ions) and exact right angles (90.0°). Within each row, the Co–Co separation is 6.5 Å. The averaged Co–N bond lengths, $[Co(py)_4(pym)_2]$ (2.2 Å) and $[Co(py)_3(pym)_3]$ (2.3 Å), suggest that the central Co atom in a $[3\times3]$ grid-like structure would possess even longer and therefore weaker bonds, resulting in a significant destabilisation of the $[3\times3]$ grid relative to the $[2\times3]$ grid. The $[3\times3]$ grid would however possess the greatest number of stabilising π–π contacts. The phenyl rings also hinder destabilising ′pinching′ effects. The formation of $[3\times3]$ grids would satisfy the "principle of maximum site occupancy", which accounts for full metal coordination as directing code, but it would introduce strong warping deformation in the structure due to the "pinching" of the coordination sites. Conversely, in the $[2\times3]$ grids the metal coordination possibilities are not fully satisfied, three potential sites being unoccupied, but much of the warping is avoided. Furthermore, whereas a $[3\times3]$ grid possesses altogether 36 unfavourable *cisoid* NC–CN conformations, a $[2\times3]$ grid of the present type has only 24 of them. It is clear that the formation of $[2\times3]$ *versus* $[3\times3]$ grid structures results from a delicate balance between opposite energetical contributions. There may also be kinetic impasses imposed by sterically demanding pyrimidine substituents, as well as possible anion templating or chaperoning effects along the reaction coordinate. In the case of ligand **1d**, the $[2\times3]$ structure may therefore represent the best compromise between maximising the number of Co–N coordination interactions while avoiding twelve unfavourable *cisoid* conformations, the poor $[Co(py)_2(pym)_4]$ coordination set, as well as much of the deformation caused by "pinching".

Conclusion

The generation of several new, multimetallic complexes of grid-type architecture was achieved by the self-assembly of a set of substituted tris-terdentate ligands **1a–d**, based on terpyridine-like subunits, and octahedrally coordinated metal ions. The structure obtained depends strongly on the ligand substituent, the metal ion, the counterion, the solvent, and the reaction conditions. Under suitable conditions, a $[3\times3]$ grid was isolated from the reaction of ligand **1a** with zinc tetrafluoroborate and of ligand **1b** with mercury triflate. The other ligands possessing larger substituents on the pyrimidines did not result in formation of $[3\times3]$ grids, but instead yielded mainly hexanuclear $[M_6L_5]^{12+}$ $[2\times3]$ and tetranuclear $[M_4L_4]^{8+}$ $[2\times2]$ grid-type complexes in varying relative proportions. The proposed $[2\times3]$ grid architecture has been unambiguously characterised on the basis of a single-crystal X-ray diffraction study. In this structure, the central pyrimidine—pyridine–pyrimidine non-coordinating sites adopt a *transoid* conformation. The much less stable *cisoid* ligand conformations, the "pinching" of the coordination sites in the complex, the weaker donor strength of the central complexation site and the steric demand of the substituents are all factors contributing to the reluctance to produce the $[3\times3]$ structure. Thus, a subtle interplay between metal coordination, strain and steric demand of the ligands as well as external factors, reaction conditions and nature of the counterion, determines the product of self-assembly. The results indicate that by tuning the reaction conditions, complexes containing six to nine octahedrally coordinated metal ions in a well defined grid-type arrangement are accessible. The difficulties in the rigorous control of the large number of parameters, however, suggest that other ligand designs and assembly procedures may have to be devised for the generation of even larger grid-type structures. Further investigations into the electronic and magnetic properties of the grid complexes obtained are currently in progress.

One may note that both types of complexes, $[2\times3]$ and $[3\times3]$, are of interest as self-assembled coordination architectures presenting arrays of transition metal ions of well-defined structure and nuclearity. In line with earlier results on $[2\times2]$ grids,[3–5] they may display a range of novel physicochemical features. Finally, by making accessible specific arrays of metal ion "dots", they contribute to the progressive build-up of a range of entities required for local addressing, pattern generation and information storage in nanostructures.[16]

Experimental Section

General: The reagents and solvents were used without further purification. In most cases, no reaction yields are given as the product was isolated by evaporation of the solvent and used directly for further investigations. The NMR data were obtained at room temperature on Bruker AC 200 at 200.1 MHz (^{1}H), on a Bruker AM 400 instrument (400 MHz) and on a Bruker Avance DRX 500 (500 MHz), calibrated against the solvent residue signal (CD_3CN: $\delta = 1.94$ ppm), and are given in ppm.

$[Zn_6(1a)_5](PF_6)_{12}$: To a suspension of **1a** (19.1 mg, 35.1 μmol) in MeOH (5 mL) was added $Zn(OAc)_2\cdot2H_2O$ (11.6 mg, 52.7 μmol). The reaction mixture was heated under reflux for 12 h. After cooling to room temperature, the reaction mixture was filtered. Excess aqueous ammonium hexafluorophosphate was added to the filtrate. The white precipitate was isolated by filtration and was washed with MeOH (2×10 mL) and H_2O (2×10 mL). The product was recrystallised from CH_3CN/diethyl ether as a pale pink solid (9.5 mg). ^{1}H NMR (400 MHz, CD_3CN): $\delta = 7.09$ (m, 2H; $H_{5''C}$), 7.24 (d, $J = 1.2$ Hz, 4H; H_{2A}), 7.25 (m, 4H; $H_{5''A}$), 7.36 (m, 4H; $H_{5''B}$), 7.62 (m, 6H $H_{6''A\text{ or }B}$), 7.72 (d, $J = 5.0$ Hz, 4H; $H_{6''A\text{ or }B}$), 7.80 (t, $J = 7.9$ Hz, 1H; $H_{4''C}$), 7.91 (t, $J = 7.9$ Hz, 2H; $H_{4''A\text{ or }B}$), 8.06 (td, $J = 7.9$, 1.2 Hz, 2H; $H_{4''C}$), 8.13 (m, 4H; $H_{4''B}$), 8.16 (m, 4H; $H_{4''A}$), 8.17 (d, $J = 1.1$ Hz, 2H; H_{2C}), 8.20 (d, $J = 1.2$ Hz, 4H; H_{2B}), 8.25 (d, $J = 7.6$ Hz, 2H; $H_{3''C}$), 8.35 (d, $J = 7.9$ Hz, 4H; $H_{3''A\text{ or }B}$), 8.55 (s, 2H; H_{2C}), 8.57 (dd, $J = 8.2$, 0.6 Hz, 4H; $H_{3''A\text{ or }B}$), 8.61 (dt, $J = 7.9$, 0.6 Hz, 2H; $H_{3''C}$), 8.70 (dt, $J = 8.2$, 0.6 Hz, 4H; $H_{3''A\text{ or }B}$), 8.89 (t, $J = 8.2$ Hz, 4H; $H_{4'A\text{ or }B}$), 8.96 (d, $J = 7.6$ Hz, 4H; $H_{A\text{ or }B}$), 9.03 (d,

  0947-6539/02/0815-3464 $ 20.00+.50/0 *Chem. Eur. J.* **2002**, *8*, No. 15

$J = 7.6$ Hz, 4H; $H_{A\ or\ B}$), 9.10 (d, $J = 7.9$ Hz, 4H; $H_{A\ or\ B}$), 9.14 (d, $J = 7.3$ Hz, 2H; H_C), 9.19 (dd, $J = 8.2$, 0.6 Hz, 2H; H_C), 9.26 (dd, $J = 8.2$, 1.1 Hz, 4H; $H_{5'B}$), 9.31 (d, $J = 7.9$ Hz, 4H; $H_{5'A}$), 9.49 (s, 2H; H_{5C}), 9.50 (d, $J = 8.5$ Hz, 4H; $H_{3'''A}$), 9.61 (d, $J = 0.9$ Hz, 4H; H_{5B}), 9.68 ppm (d, $J = 0.6$ Hz, 4H; H_{5A}).

$[Zn_6(1a)_5](OTf)_{12}$: A solution of **1a** (3 mg, 5.5 μmol) and $Zn(OTf)_2 \cdot H_2O$ (3.16 mg, 8.3 μmol) in CD_3CN (0.4 mL) was heated under reflux for 21 h. The product was isolated as a pale yellow powder by evaporation of the solvent. ^1H NMR (200 MHz, CD_3CN): mixture of compounds. MS (ESI): *m/z* (%): 1483.6 (74) $\{[Zn_6(\mathbf{1a})_5](OTf)_9\}^{3+}$, 1075.3 (100) $\{[Zn_6(\mathbf{1a})_5](OTf)_8\}^{4+}$, 940.1 (50) $\{[Zn_3(\mathbf{1a})_2](OTf)_4\}^{2+}$, 830.8 (57) $\{[Zn_6(\mathbf{1a})_5](OTf)_7\}^{5+}$, 758.3 (73) $\{[Zn(\mathbf{1a})](OTf)\}^{+}$, 667.0 (21) $\{[Zn_6(\mathbf{1a})_5](OTf)_6\}^{6+}$, 577.1 (66) $\{[Zn_4(\mathbf{1a})_4](OTf)_3\}^{5+}$, 455.7 (18) $\{[Zn_4(\mathbf{1a})_4](OTf)_2\}^{6+}$.

$[Zn_9(1a)_6](BF_4)_{18}$: A solution of **1a** (2.5 mg, 4.6 μmol) and $Zn(BF_4)_2 \cdot 8H_2O$ (2.64 mg, 6.9 μmol) in CD_3CN (0.4 mL) was heated under reflux for 19 h. The product was isolated as a pale yellow powder by evaporation of the solvent. ^1H NMR (500 MHz, CD_3CN): $\delta = 6.97$ (d, $J = 0.9$ Hz, 2H; H_{2B}), 7.02 (d, $J = 1.0$ Hz, 4H; H_{2A}), 7.11 (ddd, $J = 7.4$, 5.4, 1.0 Hz, 2H; $H_{5''B}$), 7.16 (ddd, $J = 7.5$, 5.4, 1.0 Hz, 4H; $H_{5''A}$), 7.29 (ddd, $J = 5.4$, 1.5, 0.8 Hz, 2H; $H_{6''B}$), 7.31 (ddd, $J = 5.2$, 1.5, 0.8 Hz, 4H; $H_{6''A}$), 7.92 (td, $J = 7.7$, 1.6 Hz, 2H; $H_{4''B}$), 7.94 (td, $J = 7.6$, 1.7 Hz, 4H; $H_{4''A}$), 8.26 (d, $J = 8.0$ Hz, 2H; $H_{3''B}$), 8.33 (d, $J = 8.2$ Hz, 4H; $H_{3''A}$), 8.69 (dd, $J = 4.5$, 1.2 Hz, 2H; $H_{5'B}$), 8.76 (dd, $J = 8.3$, 0.9 Hz, 4H; $H_{5'A}$), 8.82 (t, $J = 8.0$ Hz, 4H; $H_{4'A}$), 8.84 (t, $J = 8.2$ Hz, 1H; $H_{4'''B}$), 8.95 (t, $J = 4.4$ Hz, 2H; $H_{4'B}$), 9.03 (t, $J = 8.3$ Hz, 2H; $H_{4'''A}$), 9.12 (dd, $J = 7.8$, 0.8 Hz, 4H; $H_{3'A}$), 9.16 (d, $J = 0.9$ Hz, 2H; H_{5B}), 9.17 (d, $J = 8.2$ Hz, 2H; $H_{3'''B}$), 9.28 (d, $J = 8.2$ Hz, 4H; $H_{3'''A}$), 9.35 ppm (d, $J = 0.9$ Hz, 2H; H_{5A}); MS (ESI): *m/z* (%): 1716.6 (18) $\{[Zn_9(\mathbf{1a})_6](BF_4)_{15}\}^{3+}$, 1265.0 (42) $\{[Zn_9(\mathbf{1a})_6](BF_4)_{14}\}^{4+}$, 995.6 (71) $\{[Zn_9(\mathbf{1a})_6](BF_4)_{13}\}^{5+}$, 814.9 (100) $\{[Zn_9(\mathbf{1a})_6](BF_4)_{12}\}^{6+}$, 686.1 (49) $\{[Zn_9(\mathbf{1a})_6](BF_4)_{11}\}^{7+}$, 589.3 (19) $\{[Zn_9(\mathbf{1a})_6](BF_4)_{10}\}^{8+}$.

Reaction of 1b with $Cu(OTf)_2$: $Cu(OTf)_2$ (3.6 mg, 9.8 μmol) was added to a suspension of **1b** (5 mg, 6.5 μmol) in $CH_3CN/CHCl_3$ (6:1, 0.7 mL). The resulting solution was stirred at room temperature for two days. The solvent was evaporated and the product recrystallised from acetonitrile/diethyl ether to yield a pale green solid. MS (ESI): *m/z* (%): 1352.1 (26) $\{[Cu_6(\mathbf{1b})_5](OTf)_8\}^{4+}$, 1051.4 (52) $\{[Cu_6(\mathbf{1b})_5](OTf)_7\}^{5+}$, 978.9 (8) $\{[Cu_4(\mathbf{1b})]_4(OTf)_4\}^{4+}$, 850.9 (56) $\{[Cu_6(\mathbf{1b})_5](OTf)_6\}^{6+}$, 752.8 (24) $\{[Cu_4(\mathbf{1b})_4](OTf)_3\}^{5+}$, 595.0 (45) no assignment found, 373.6 (85) no assignment found, 262.8 (100) no assignment found.

$[Co_6(1b)_5](OTf)_{12}$: A solution of $[Co(DMSO)_6](OTf)_2$ (8.1 mg, 9.8 μmol) in CH_3CN (0.5 mL) was added to a suspension of **1b** (5 mg, 6.5 μmol) in CH_3CN (3 mL). The mixture was heated under reflux for 48 h. Evaporation of the solvent gave the product as a brown powder, which was recrystallised from CH_3CN/diethyl ether. ^1H NMR (200 MHz, CD_3CN): $\delta = 3.5$, 4.8, 5.2, 5.8, 7.0, 8.0, 10.0, 10.2, 11.1, 12.1, 12.6, 14.1, 14.9, 15.8, 16.2, 22.1, 26.4, 28.4, 36.3, 40.0, 41.2, 52.7, 55.3, 57.5, 59.1, 61.7, 63.2, 67.4, 68.8, 69.7, 72.0, 80.1, 101.4, 134.9 ppm; MS (ESI): *m/z* (%): 1842.3 (10) $\{[Co_6(\mathbf{1b})_5](OTf)_9\}^{3+}$, 1344.3 (32) $\{[Co_6(\mathbf{1b})_5](OTf)_8\}^{4+}$, 1045.7 (65) $\{[Co_6(\mathbf{1b})_5](OTf)_7\}^{5+}$, 974.0 (5) $\{[Co_4(\mathbf{1b})_4](OTf)_4\}^{4+}$, 846.5 (100) $\{[Co_6(\mathbf{1b})_5](OTf)_6\}^{6+}$, 749.3 (34) $\{[Co_4(\mathbf{1b})_4](OTf)_3\}^{5+}$, 704.0 (38) $\{[Co_6(\mathbf{1b})_5](OTf)_5\}^{7+}$, 599.6 (30) $\{[Co_6(\mathbf{1b})_5](OTf)_4\}^{8+}$ and $\{[Co_4(\mathbf{1b})_4](OTf)_2\}^{6+}$, 492.5 (10) $\{[Co_4(\mathbf{1b})_4](OTf)\}^{7+}$, 412.4 (8) $\{[Co_4(\mathbf{1b})_4]\}^{8+}$.

$[Hg_9(1b)_6](OTf)_{18}$: A mixture of $Hg(OTf)_2$ (11.23 mg, 22 μmol) and **1b** (11.5 mg, 15 μmol) in CH_3CN (3 mL) was stirred at room temperature under a N_2 atmosphere overnight. The solvent was removed to yield a pale yellow solid that was recrystallised from CH_3CN/diethyl ether. ^1H NMR (200 MHz, CD_3CN; due to insufficient resolution, the coupling constants could not be determined): $\delta = 1.4$–1.1 (m, 27H), 2.2–1.7 (m, 18H), 3.8–3.2 (m, 18H), 7.35–7.15 (m, 12H), 7.81 (t, 2H), 7.91 (t, 4H), 8.10 (s, 2H), 8.15 (d, 2H), 8.33 (s, 4H), 8.37 (d, 4H), 8.43 (s, 4H), 8.64 (s, 2H), 8.71 (s, 2H), 8.77 (s, 2H), 8.93 (s, 4H), 9.10 (s, 4H), 9.24 (s, 2H), 9.52 (s, 4H); MS (ESI): *m/z* (%): 2128.5 (27) $\{[Hg_9(\mathbf{1b})_6](OTf)_{14}\}^{4+}$, 1672.2 (70) $\{[Hg_9(\mathbf{1b})_6](OTf)_{13}\}^{5+}$, 1368.2 (100) $\{[Hg_9(\mathbf{1b})_6](OTf)_{12}\}^{6+}$, 1150.9 (60) $\{[Hg_9(\mathbf{1b})_6](OTf)_{11}\}^{7+}$, 987.9 (21) $\{[Hg_9(\mathbf{1b})_6](OTf)_{10}\}^{8+}$, 861.2 (6) $\{[Hg_9(\mathbf{1b})_6](OTf)_9\}^{9+}$.

Reaction of $Co(BF_4)_2 \cdot 6H_2O$ with 1c in acetonitrile: A solution of **1c** (2.5 mg, 4.4 μmol) and $Co(BF_4)_2 \cdot 6H_2O$ (2.23 mg, 6.6 μmol) in CD_3CN (0.5 mL) was heated under reflux for 5.5 days. The product was isolated as brown powder by evaporation of the solvent. ^1H NMR (200 MHz, CD_3CN): mixture of compounds. MS (ESI): *m/z* (%): 1331.0 (20) $\{[Co_6(\mathbf{1c})_5](BF_4)_9\}^{3+}$, 976.3 (80) $\{[Co_6(\mathbf{1c})_5](BF_4)_8\}^{4+}$, 763.5 (94) $\{[Co_6(\mathbf{1c})_5](BF_4)_7\}^{5+}$, 717.0 (28) $\{[Co_4(\mathbf{1c})_4](BF_4)_4\}^{4+}$, 621.7 (14) $\{[Co_6(\mathbf{1c})_5](BF_4)_6\}^{6+}$, 556.2 (100) $\{[Co_4(\mathbf{1c})_4](BF_4)_4\}^{5+}$.

Reaction of $Co(BF_4)_2 \cdot 6H_2O$ with 1c in benzonitrile: A suspension of **1c** (2.5 mg, 4.4 μmol) and $Co(BF_4)_2 \cdot 6H_2O$ (2.2 mg, 6.6 μmol) in benzonitrile (0.5 mL) was heated to 180 °C for 67 h. After the mixture had been cooled to room temperature, the complex was precipitated and washed with Et_2O to yield a pale brown powder. ^1H NMR (200 MHz, CD_3CN): $\delta = -115.9$, -73.1, -11.1, ?8.7, 7.8, 8.9, 14.5, 20.3, 27.8, 28.2, 30.8, 47.0, 51.2, 53.0, 54.4, 61.1, 65.9, 69.6, 98.2, 99.8, 105.5, 117.6; MS (ESI): *m/z* (%): 1331.0 (5) $\{[Co_6(\mathbf{1c})_5](BF_4)_9\}^{3+}$, 976.8 (32) $\{[Co_6(\mathbf{1c})_5](BF_4)_8\}^{4+}$, 764.2 (73) $\{[Co_6(\mathbf{1c})_5](BF_4)_7\}^{5+}$, 919.7 (5) $\{[Co_4(\mathbf{1c})_4](BF_4)_4\}^{4+}$, 622.6 (100) $\{[Co_6(\mathbf{1c})_5](BF_4)_6\}^{6+}$, 557.1 (67) $\{[Co_4(\mathbf{1c})_4](BF_4)_3\}^{5+}$.

Reaction of $Fe(BF_4)_2 \cdot 6H_2O$ with 1c in acetonitrile: A solution of ligand **1c** (2 mg, 3.5 μmol) and $Fe(BF_4)_2 \cdot 6H_2O$ (1.77 mg, 5.3 μmol) in CD_3CN (0.5 mL) was heated under reflux for 5.5 days. The product was isolated as a dark blue powder by evaporation of the solvent. ^1H NMR (200 MHz, CD_3CN): mixture of products. MS (ESI): *m/z* (%): 1324.9 (4) $\{[Fe_6(\mathbf{1c})_5](BF_4)_9\}^{3+}$, 971.7 (8) $\{[Fe_6(\mathbf{1c})_5](BF_4)_8\}^{4+}$, 714.0 (61) $\{[Fe_4(\mathbf{1c})_4](BF_4)_4\}^{4+}$, 553.7 (100) $\{[Fe_4(\mathbf{1c})_4](BF_4)_3\}^{5+}$ and further signals, which cannot be assigned.

Reaction of $Fe(BF_4)_2 \cdot 6H_2O$ with 1c in benzonitrile: A suspension of **1c** (2 mg, 3.5 μmol) and $Fe(BF_4)_2 \cdot 6H_2O$ (1.77 mg, 5.3 μmol) in benzonitrile (0.5 mL) was heated to 180 °C for 66 h. After the mixture had been cooled to room temperature, the complex was precipitated and washed with Et_2O to yield a dark blue powder. ^1H NMR (200 MHz, CD_3CN): $\delta = -27.3$, -24.8, -5.4, 5.3, 5.8, 6.5, 8.0, 8.9, 9.5, 9.8, 10.1, 10.4, 11.8, 13.7, 14.6, 15.8, 21.0, 52.5, 60.1, 61.7, 63.8, 69.6, 75.3;MS (ESI): *m/z* (%): 1324.9 (4) $\{[Fe_6(\mathbf{1c})_5](BF_4)_9\}^{3+}$, 972.2 (25) $\{[Fe_6(\mathbf{1c})_5](BF_4)_8\}^{4+}$, 760.5 (65) $\{[Fe_6(\mathbf{1c})_5](BF_4)_7\}^{5+}$, 714. (14) $\{[Fe_4(\mathbf{1c})_4](BF_4)_4\}^{4+}$, 619.5 (84) $\{[Fe_6(\mathbf{1c})_5](BF_4)_6\}^{6+}$, 554.6 (100) $\{[Fe_4(\mathbf{1c})_4](BF_4)_3\}^{5+}$.

Reaction of $Zn(OTf)_2 \cdot H_2O$ with 1c: A solution of **1c** (2.00 mg, 3.5 μmol) and $Zn(OTf)_2 \cdot H_2O$ (2.00 mg, 5.3 μmol) in CD_3CN (0.4 mL) was heated under reflux for 5.5 days. The product was isolated as a pale yellow powder by evaporation of the solvent. ^1H NMR (200 MHz, CD_3CN): mixture of products. MS (ESI): *m/z* (%): 1530.7 (6) $\{[Zn_6(\mathbf{1c})_5](OTf)_9\}^{3+}$, 1110.5 (13) $\{[Zn_6(\mathbf{1c})_5](OTf)_8\}^{4+}$, 967.4 (7) $\{[Zn_3(\mathbf{1c})_2](OTf)_4\}^{2+}$, 858.2 (8) $\{[Zn_6(\mathbf{1c})_5](OTf)_7\}^{5+}$, 785.6 (33) $\{[Zn(\mathbf{1c})](OTf)\}^{+}$, 584.0 (100) no assignment found.

Reaction of $Zn(BF_4)_2 \cdot 8H_2O$ with 1c: A solution of **1c** (2.50 mg, 4.4 μmol) and $Zn(BF_4)_2 \cdot 8H_2O$ (2.51 mg, 6.6 μmol) in CD_3CN (0.4 mL) was heated under reflux for 19 h. The product was isolated as a pale yellow powder by evaporation of the solvent. ^1H NMR (200 MHz, CD_3CN): mixture of products. MS (ESI): *m/z* (%): 1343.1 (13) $\{[Zn_6(\mathbf{1c})_5](BF_4)_9\}^{3+}$, 986.0 (41) $\{[Zn_6(\mathbf{1c})_5](BF_4)_8\}^{4+}$, 771.2 (100) $\{[Zn_6(\mathbf{1c})_5](BF_4)_7\}^{5+}$, 723.3 (44) $\{[Zn_4(\mathbf{1c})_4](BF_4)_4\}^{4+}$, 627.8 (51) $\{[Zn_6(\mathbf{1c})_5](BF_4)_6\}^{6+}$, 561.7 (88) $\{[Zn_4(\mathbf{1c})_4](BF_4)_3\}^{5+}$, 453.2 (23) $\{[Zn_4(\mathbf{1c})_4](BF_4)_2\}^{6+}$.

Reaction of $Co(BF_4)_2 \cdot 6H_2O$ with 1d in acetonitrile: A solution of **1d** (3 mg, 4.3 μmol) and $Co(BF_4)_2 \cdot 6H_2O$ (2.20 mg, 6.5 μmol) in CD_3CN (0.4 mL) was heated under reflux for 67 h. The product was isolated as a brown powder by evaporation of the solvent. ^1H NMR (200 MHz, CD_3CN): mixture of products, broad signals. MS (ESI): *m/z* (%): 1537.0 (19) $\{[Co_6(\mathbf{1d})_5](BF_4)_9\}^{3+}$, 1305.1 (23) $\{[Co_6(\mathbf{1d})_6](BF_4)_8\}^{4+}$, 1131.3 (41) $\{[Co_6(\mathbf{1d})_5](BF_4)_8\}^{4+}$, 1026.8 (27) $\{[Co_6(\mathbf{1d})_6](BF_4)_7\}^{5+}$, 887.8 (45) $\{[Co_6(\mathbf{1d})_5](BF_4)_7\}^{5+}$, 841.3 (100) $\{[Co(\mathbf{1d})](BF_4)\}^{+}$ and $\{[Co_6(\mathbf{1d})_6](BF_4)_6\}^{6+}$, 725.3 (64) $\{[Co_6(\mathbf{1d})_5](BF_4)_6\}^{6+}$, 708.8 (34) $\{[Co_6(\mathbf{1d})_6](BF_4)_5\}^{7+}$, 609.3 (46) $\{[Co_6(\mathbf{1d})_5](BF_4)_5\}^{7+}$ and $\{[Co_6(\mathbf{1d})_6](BF_4)_4\}^{8+}$, 531.9 (32) $\{[Co_6(\mathbf{1d})_6](BF_4)_3\}^{9+}$, 377.6 (29) $\{[Co(\mathbf{1d})]\}^{2+}$.

Reaction of $Co(BF_4)_2 \cdot 6H_2O$ with 1d in benzonitrile: $[Co_6(1d)_5](BF_4)_{12}$: A suspension of **1d** (3 mg, 4.3 μmol) and $Co(BF_4)_2 \cdot 6H_2O$ (2.20 mg, 6.5 μmol) in benzonitrile (0.4 mL) was heated to 180 °C for 30 h. After the mixture had been cooled to room temperature, the complex was precipitated and washed with Et_2O to give $[Co_6(\mathbf{1d})_5](BF_4)_{12}$ as a pale brown powder (3.7 mg). ^1H NMR (200 MHz, CD_3CN): $\delta = -113.5$, -69.0, -66.4, -14.4, -10.1, -8.9, -8.3, -2.7, 4.5, 7.2, 9.1, 19.6, 25.4, 27.0, 27.6, 38.7, 40.6, 46.5, 49.4, 51.3, 55.2, 57.6, 69.9, 70.7, 76.7, 80.4, 96.2, 99.7, 110.9, 124.5, 129.2, 136.7; MS (ESI): *m/z* (%): 1537.0 (18) $\{[Co_6(\mathbf{1d})_5](BF_4)_9\}^{3+}$, 1131.3 (60) $\{[Co_6(\mathbf{1d})_5](BF_4)_8\}^{4+}$, 887.8 (100) $\{[Co_6(\mathbf{1d})_5](BF_4)_7\}^{5+}$, 841.7 (2) $\{[Co_4(\mathbf{1d})_4](BF_4)_4\}^{4+}$, 725.4 (79) $\{[Co_6(\mathbf{1d})_5](BF_4)_6\}^{6+}$, 655.8 (18)

$\{[Co_4(\mathbf{1d})_4](BF_4)_3\}^{5+}$, 609.5 (38) $\{[Co_6(\mathbf{1d})_5](BF_4)_5\}^{7+}$, 532.0 (17) $\{[Co_4(\mathbf{1d})_4](BF_4)_4\}^{6+}$.

Reaction of $Fe(BF_4)_2\cdot 6H_2O$ with 1d in acetonitrile: A solution of **1d** (3.00 mg, 4.3 μmol) and $Fe(BF_4)_2\cdot 6H_2O$ (2.18 mg, 6.5 μmol) in CD_3CN (0.4 mL) was heated under reflux for 67 h. The product was isolated as a dark purple powder by evaporation of the solvent. ^1H NMR (200 MHz, CD_3CN): very broad signals. MS (ESI): *m/z* (%): 1762.8 (2) $\{[Fe_6(\mathbf{1d})_6](BF_4)_9\}^{3+}$, 1531.7 (2) $\{[Fe_6(\mathbf{1d})_5](BF_4)_9\}^{7+}$, 1300.5 (7) $\{[Fe_6(\mathbf{1d})_6](BF_4)_8\}^{4+}$, 1022.9 (14) $\{[Fe_6(\mathbf{1d})_6](BF_4)_7\}^{5+}$, 883.9 (5) $\{[Fe_6(\mathbf{1d})_5](BF_4)_7\}^{5+}$, 838.1 (91) $\{[Fe_6(\mathbf{1d})_6](BF_4)_6\}^{6+}$ and $\{[Fe(\mathbf{1d})](BF_4)\}^{+}$, 706.1 (36) $\{[Fe_6(\mathbf{1d})_6](BF_4)_5\}^{7+}$, 606.9 (57) $\{[Fe_6(\mathbf{1d})_6](BF_4)_4\}^{8+}$, 529.8 (3) $\{[Fe_6(\mathbf{1d})_6](BF_4)_3\}^{9+}$, 468.3 (25) $\{[Fe_6(\mathbf{1d})_6](BF_4)_2\}^{10+}$, 376.0 (100) $\{[Fe(\mathbf{1d})]\}^{2+}$.

Reaction of $Fe(BF_4)_2\cdot 6H_2O$ with 1d in benzonitrile: $[Fe_6(1d)_5](BF_4)_{12}$: A solution of **1d** (3 mg, 4.3 μmol) and $Fe(BF_4)_2\cdot 6H_2O$ (2.2 mg, 6.5 μmol) in benzonitrile (0.5 mL) was heated to 180 °C for 20 h. After the mixture had been cooled to room temperature, the complex was precipitated and washed with Et_2O to give a dark blue-grey powder. ^1H NMR (200 MHz, CD_3CN): $\delta = -23.0, -17.3, -13.2, -9.7, -7.4, -4.5, -2.4, -1.9, 5.6, 7.6, 8.8, 9.5, 10.2, 10.6, 14.3, 15.4, 25.0, 47.1, 49.3, 53.6, 54.6, 59.6, 60.5, 65.3, 66.6, 72.8, 78.3, 81.9$; MS (ESI): *m/z* (%): 1531.8 (4) $\{[Fe_6(\mathbf{1d})_5](BF_4)_9\}^{3+}$, 1127.2 (17) $\{[Fe_6(\mathbf{1d})_5](BF_4)_8\}^{4+}$, 884.6 (44) $\{[Fe_6(\mathbf{1d})_5](BF_4)_7\}^{5+}$, 722.9 (100) $\{[Fe_6(\mathbf{1d})_5](BF_4)_6\}^{6+}$, 607.4 (54) $\{[Fe_6(\mathbf{1d})_5](BF_4)_5\}^{7+}$.

X-ray structural analysis of $[Co_6(1d)_5](BF_4)_{12}$: X-ray diffraction measurements were carried out at 120 K at beamline ID11 at the European Synchrotron Radiation Facility. A wavelength of 0.51593 Å was selected by using a double crystal Si(111) monochromater, and data were collected by using a Bruker Smart CCD-camera system. The camera was held at fixed 2θ, while the sample was rotated over 0.2° intervals during 1 second exposures. Data were integrated with Bruker SAINT software to produce *hkl* versus $|F|^2$ suitable for structure solution via direct methods. $[C_{225}H_{145}N_{45}Co_6]^{12+}\cdot 12\,BF_4^-$, $M_r = 5063.58$, orthorhombic $Cmc2_1$, $a = 32.101(6)$, $b = 15.995(3)$, $c = 49.957(9)$ Å, $V = 25651(8)$ Å^3, $\mu(Mo_{K\alpha}) = 0.471$ mm^{-1} (based on found atoms, see below), $Z = 4$, $\rho_{calcd} = 1.311$ g cm^{-3}, $F(000) = 10244$, $T = 120$ K. A total of 115936 collected reflections, 20976 unique reflections [14937 $I > 2\sigma(I)$] were used for refinement. Structure solution was done by direct methods[16] and refinement on F^2.[17] The hydrogen atoms were calculated to their idealised positions with isotropic temperature factors (1.2 or 1.5 times the C temperature factor) and were refined as riding atoms. Eighteen geometrical DFIX restraints were needed to make some of the aromatic rings and four BF_4^- ions chemically reasonable. The remaining aromatic rings of the grid were constrained to the regular hexagons. Altogether five temperature factors were equalised. One fluorine in one BF_4^- is disordered (occupancy 0.5) over two orientations. All the BF_4^- ions and two aromatic rings of the grid were refined isotropically due to bad crystal data. One BF_4^- ion could not be located at all. The residual electron density was modelled as 23 carbon atoms, because it was not possible to arrive at a reliable model for probable, but badly disordered BF_4^- ion and solvent molecules. However in the end, the convergence of the structure refinement was good (shift/error < 0.01). The final *R* values were $R = 0.1932$, $wR^2 = 0.5043$ [$I > 2\sigma(I)$], $R = 0.2451$, $wR^2 = 0.5583$ (all data) for 265 parameters, Goodness-of-fit on $F^2 = 2.359$. A final difference map displayed the highest electron density of 2.72 eÅ^{-3}, which is located near to constrained aromatic rings and disordered isotropic BF_4^- anions. CCDC-180277 contains the supplementary crystallographic data (excluding structure factors) for the structure reported in this paper. These data can be can be obtained free of charge via www.ccdc.cam.ac.uk/conts/retrieving.html (or from the Cambridge Crystallographic Data Centre, 12 Union Road, Cambridge CB2 1EZ, UK; fax: (+44) 1223-336033; or deposit@ccdc.cam.ac.uk).

Acknowledgement

We thank P. Maltèse and S. P. Smidt for recording the COSY, ROESY and NOESY NMR spectra. F.J.R.-S. thanks the Ministry of Education and Culture of Spain for a postdoctoral fellowship. A.M.G. thanks the University of Santiago de Compostela and the TMR programme of the European Union for postdoctoral fellowships. A graduate fellowship from the "Ministère de l'Education Nationale, de la Recherche et de la Technologie" (E.B.) and financial support of the Natural Sciences and Engineering Research Council of Canada NSERC (G.S.H.), the Finnish Ministry of Education (E.W.), and the Collège de France (P.N.W.B.) are gratefully acknowledged. We thank the European Synchrotron Research Foundation for attribution of beam time and Dr. G. Vaughan for collecting the crystal data sets.

[1] a) J.-M. Lehn, *Supramolecular Chemistry: Concepts and Perspectives*, VCH, Weinheim, **1995**, chapter 9; b) G. F. Swiegers, T. J. Malefetse, *Chem. Rev.* **2000**, *100*, 3483—3537; c) P. N. W. Baxter in *Comprehensive Supramolecular Chemistry*, *Vol. 9* (Eds.: J. L. Atwood, J. E. D. Davies, D. D. MacNicol, F. Vögtle, J.-M. Lehn), Oxford, **1996**, pp. 254 – 282; d) M. Fujita in *Comprehensive Supramolecular Chemistry*, *Vol. 9* (Eds.: J. L. Atwood, J. E. D. Davies, D. D. MacNicol, F. Vögtle, J.-M. Lehn), Oxford, **1996**, pp. 253 – 282; e) D. Philp, J. F. Stoddart, *Angew. Chem.* **1996**, *108*, 1242 – 1286; *Angew. Chem. Int. Ed. Engl.* **1996**, *35*, 1154.

[2] a) M.-T. Youinou, N. Rahmouni, J. Fischer, J. A. Osborn, *Angew. Chem.* **1992**, *104*, 771 – 773; *Angew. Chem. Int. Ed. Engl.* **1992**, *31*, 733 – 735; b) P. N. W. Baxter, J.-M. Lehn, J. Fischer, M.-T. Youniou, *Angew. Chem.* **1994**, *106*, 2432 – 2434; *Angew. Chem. Int. Ed. Engl.* **1994**, *33*, 2284—2287; c) P. N. W. Baxter, R. G. Khoury, J.-M. Lehn, G. Baum, D. Fenske, *Chem. Eur. J.* **2000**, *6*, 4140 – 4148; d) G. S. Hanan, D. Volkmer, U. S. Schubert, J.-M. Lehn, G. Baum, D. Fenske, *Angew. Chem.* **1997**, *109*, 1929 – 1931; *Angew. Chem. Int. Ed. Engl.* **1997**, *36*, 1842 – 1844.

[3] M. Ruben, E. Breuning, J.-P. Gisselbrecht, J.-M. Lehn, *Angew. Chem.* **2000**, *112*, 4312—4315; *Angew. Chem. Int. Ed.* **2000**, *39*, 4139 – 4142.

[4] a) O. Waldmann, J. Hassmann, P. Müller, G. S. Hanan, D. Volkmer, U. S. Schubert, J.-M. Lehn, *Phys. Rev. Lett.* **1997**, *78*, 3390—3393; b) E. Breuning. M. Ruben, J.-M. Lehn, F. Renz, Y. Garcia, V. Ksenofontov, P. Gütlich, E. Wegelius, K. Rissanen, *Angew. Chem.* **2000**, *112*, 2563 – 2566; *Angew. Chem. Int. Ed.* **2000**, *39*, 2504 – 2507.

[5] J. Rojo, F. J. Romero-Salguero, J.-M. Lehn, G. Baum, D. Fenske, *Eur. J. Inorg. Chem.* **1999**, 1421 – 1428.

[6] A. Semenov, J. P. Spatz, M. Möller, J.-M. Lehn, B. Sell, D. Schubert, C. H. Weidl, U. S. Schubert, *Angew. Chem.* **1999**, *111*, 2701 – 2705; *Angew. Chem. Int. Ed.* **1999**, *38*, 2547 – 2550.

[7] L. Zhao, C. J. Matthes, L. K. Thompson, S. L. Heath, *Chem. Commun.* **2000**, 265 – 266; L. Zhao, W. Xu, L. K. Thompson, S. L. Heath, D. O. Miller, M. Ohba, *Angew. Chem.* **2000**, *112*, 3244 – 3247; *Angew. Chem. Int. Ed.* **2000**, *39*, 3114 – 3117.

[8] A. M. Garcia, F. J. Romero-Salguero, J.-M. Lehn, G. Baum, D. Fenske, *Chem. Eur. J.* **1999**, *6*, 1803 – 1808.

[9] a) G. S. Hanan, U. S. Schubert, D. Volkmer, E. Rivière, J.-M. Lehn, N. Kyritsakas, J. Fischer, *Can. J. Chem.* **1997**, *75*, 169 – 182; b) D. Bassani, J.-M. Lehn, *Bull. Soc. Chim. Fr.* **1997**, *134*, 897 – 906.

[10] For the first example of a $[m \times n]$ $(m \neq n)$ grid: P. N. W. Baxter, J.-M. Lehn, B. O. Kneisel, *Angew. Chem.* **1997**, *109*, 2067 – 2070; *Angew. Chem. Int. Ed. Engl.* **1997**, *36*, 1978 – 1981.

[11] S. T. Howard, *J. Am. Chem. Soc.* **1996**, *118*, 10269 – 10274.

[12] A. Göller, U.-W. Grummt, *Chem. Phys. Lett.* **2000**, *321*, 399.

[13] B. Hasenknopf, J.-M. Lehn, B. O. Kneisel, G. Baum. D. Fenske, *Angew. Chem.* **1996**, *108*, 1987 – 1990; *Angew. Chem. Int. Ed. Engl.* **1996**, *35*, 1838 – 1840.

[14] J. E. Huheey, E. A. Keiter, R. L. Keiter, *Inorganic Chemistry - Principles of Structure and Reactivity*, Harper Collins College Publishers, 4th edition, New York, **1993**, pp. 114 – 117.

[15] G. S. Hanan, C. R. Arana, J.-M. Lehn, G. Baum, D. Fenske, *Chem. Eur. J.* **1996**, *2*, 1292 – 1302.

[16] The $[2 \times 3]$ arrays present two sets of respectively two and four identical metal ions devided into two separately addressable subsets; see also, the $[4 \times 5]$ Ag^+_{20} grid containing two separate sets of ten silver ions.[2c] The $[3 \times 3]$ arrays possess three sets of respectively four, four, and one metal ions. The metal ions in different sets should for instance have different redox properties. See also reference [1a], p. 200.

[17] G. M. Sheldrick, SHELX-97, Universität Göttingen, **1997**.

Received: March 4, 2002 [F3920]

